Check for updates

Received: 31 January 2023 | Revised: 31 July 2023 | Accepted: 3 October 2023

DOI: 10.1111/jfr3.12958

ORIGINAL ARTICLE

CIWEM Chartered Institution of Water and Environmental Management | Journal of Flood Risk Management | WILEY

Towards new design rainfall profiles for the United Kingdom

Roberto Villalobos Herrera[1] | **Stephen Blenkinsop**[1] | **Selma B. Guerreiro**[1] | **Murray Dale**[2] | **Duncan Faulkner**[2] | **Hayley J. Fowler**[1,3]

[1]School of Engineering, Newcastle University, Newcastle upon Tyne, UK

[2]JBA Consulting, Skipton, UK

[3]Tyndall Centre for Climate Change Research, Newcastle University, Newcastle upon Tyne, UK

Correspondence
Roberto Villalobos Herrera, School of Engineering, Newcastle University, Newcastle upon Tyne, NE1 7RU, UK.
Email: roberto.villalobosherrera@ucr.ac.cr

Present address
Roberto Villalobos Herrera, School of Civil Engineering, Universidad de Costa Rica, San José, Costa Rica.

Funding information
FP7 Ideas: European Research Council, Grant/Award Number: ERC-2013-CoG-617329; Natural Environment Research Council, Grant/Award Numbers: NE/R01079X/1, NE/S017348/1, NE/V004166/1; Universidad de Costa Rica, Grant/Award Number: OAICE-CAB-OQ-150-20I6; School of Engineering of Newcastle University; UKWIR project, Grant/Award Number: 22/CL/10/19

Abstract

The Flood Studies Report (FSR) summer and winter design profiles are a key component of rainfall design guidance in the United Kingdom (UK). We have examined the rainfall profiles of over 70,000 extreme rainfall events with the original FSR profile methodology. This analysis reveals that rainfall profiles change with rainstorm duration but not season, contradicting one of the key assumptions in current UK rainfall design guidance. By using a method that does not artificially generate symmetrical and centred profiles we show that profile shapes are highly variable and strongly related to event duration and magnitude. Short events tend towards front-loaded profiles, while heavy long-duration events tend towards centred profile shapes. Finally, manual, automatic and mixed methods of deriving new design profiles for use in the UK were trialled, with consistent results. These could be used to derive new design profiles to supersede the FSR profiles. Notably, peak intensities in observed profiles and trialled summary profiles often exceeded those found in both FSR profiles. We conclude that current design profile guidance for the UK fails to account for the observed variability in event profile shapes and peak intensities and may lead to significant under- or over-design of flood risk management solutions.

KEYWORDS

design profiles, extreme events, flood estimation, flooding, hyetographs, modelling, rainfall, rainfall–runoff

1 | INTRODUCTION

Hydrosystems modelling for design, analysis and performance evaluations often rely on rainfall information as a key input. In an event-based approach, this information usually consists of a total depth or volume (V), duration (D) and a hyetograph or rainfall profile which describes the temporal variation of rainfall intensity within the event. Event profiles can be *observed* (derived from real events) or *synthetic* (conceptually derived or averaged from multiple observations), and it is common practice to rely on different profiles for different design situations. In the UK, the Flood Estimation Handbook, FEH (Institute of Hydrology, 1999), and other design guidance documents

This is an open access article under the terms of the Creative Commons Attribution License, which permits use, distribution and reproduction in any medium, provided the original work is properly cited.
© 2023 The Authors. *Journal of Flood Risk Management* published by Chartered Institution of Water and Environmental Management and John Wiley & Sons Ltd.

recommend the use of two synthetic profiles for most UK rainfall–runoff flood estimates and for the design of urban drainage systems (CIWEM, 2016; Environment Agency, 2022; SEPA, 2019; Woods Ballard et al., 2015). These are the *50% summer profile* and the *75% winter profile* (Figure 1), which were derived from a small set of events by the Flood Studies Report, FSR (NERC, 1975). Both profiles are centred, symmetric and originally recommended for use with any rainfall duration, excepting reservoir safety studies where critical storm durations exceed a few days (Institution of Civil Engineers, 2015).

Worldwide a wide variety of design profiles exist, and their use is commonly tied to different rainfall design methods. Uniform intensity profiles used in the Rational Method or the Modified Rational method (see e.g., Butler & Davies, 2011) have been widely used in urban settings. Synthetic profiles are avoided in the latest iteration of Australian Rainfall and Runoff which uses ensembles of observed profiles instead (J. Ball et al., 2019). Rainfall mass curves, otherwise known as dimensionless profiles, are widely used as a method to derive synthetic profiles from observed events (Bonnin et al., 2011; Huff, 1967; United States Department of Agriculture, 1986; Wu et al., 2006; Yin et al., 2014); this includes the FSR summer and winter profiles (NERC, 1975). A key difference between UK profiles and those used elsewhere is that they are centred: their peak intensity is in the middle of the event (Figure 1). Other important methods include the Average Variability Method (Cordery et al., 1983) and triangular profiles (Chow et al., 1988; Yen & Chow, 1983).

Profile shape, especially the timing of peak rainfall intensity within a profile, has been identified as a key variable that modifies the hydrological response (including peak runoff rates and their timing, as well as runoff volumes) of catchments to rainfall events, especially in urban settings and catchments under 2000 km^2 (J. E. Ball, 1994; Hettiarachchi et al., 2018; Lambourne & Stephenson, 1987; Müller et al., 2017; Nguyen et al., 2010; Pochwat et al., 2017; Yi Ng et al., 2020; Zhu et al., 2018). The use of a centred profile family in UK rainfall design guidance can therefore be considered as a constraint which may artificially limit the robustness of engineering designs to rainfall events with different profile shapes which may generate higher peak flows and runoff volumes, the latter of which are especially important for the design of storage systems.

This study's aim is to explore UK rainfall profiles and their characteristics compared to current design profiles. We use a large dataset of observed annual maximum-generating rainstorms (Villalobos Herrera, et al., submitted) to examine the FSR profile methodology and compare it with un-centred profiles (Section 2.). The FSR method results are presented first (Section 3.1), we then examine the influence of multiple rainfall event characteristics on the frequency of different dimensionless profile shapes (Section 3.2). Following this, three methods for generating alternative synthetic design profiles are assessed using the same dataset (Section 3.3). We discuss our findings and discuss the implications of our findings for UK rainfall design methods (Section 4.) before presenting our conclusions and recommendations (Section 5.)

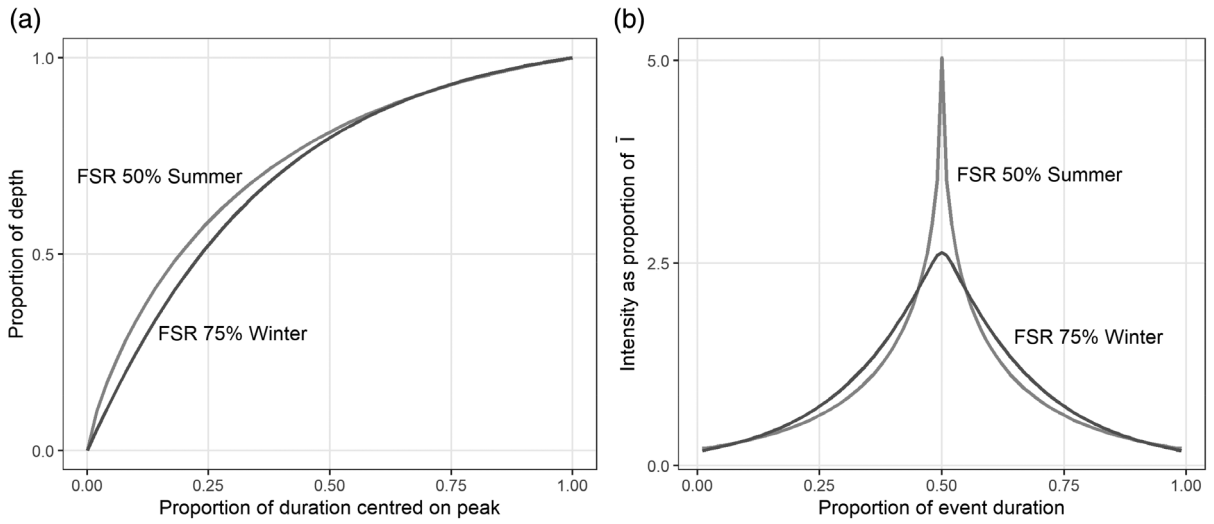

FIGURE 1 FSR/FEH storm profiles for the 50% most peaked summer storm and the 75% most peaked winter storm drawn as (a) cumulative profiles calculated using the design storm profile formula $y = \frac{1-a^z}{1-a}$, and where $z = x^b$ from Faulkner (1999) and (b) profiles showing the proportion of event duration against intensity as a proportion of mean event intensity, $\bar{I}$. Values of (a) and (b) for each profile are given in Table S1. Note that small x intervals can result in unrealistically large peak intensities for the summer profile, an interval size of 0.02 has been used to prepare these figures to match the peak intensity shown in Faulkner (1999).

1753318x, 0, Downloaded from https://onlinelibrary.wiley.com/doi/10.1111/jfr3.12958 by Newcastle University, Wiley Online Library on [08/11/2023]. See the Terms and Conditions (https://onlinelibrary.wiley.com/terms-and-conditions) on Wiley Online Library for rules of use; OA articles are governed by the applicable Creative Commons License

2 | DATA AND METHODS

2.1 | Data

Rain gauge data was provided by Environment Agency (EA), Natural Resources Wales (NRW) and the Scottish Environment Protection Agency (SEPA), and quality-controlled according to the methods described in Lewis et al. (2021) and extended in Villalobos Herrera et al. (2022). Sub-hourly data (tip-time or 15-min accumulations) was used to discern the rapid variations in rainfall intensity that may occur in heavy short-duration rainstorms. The resulting 1279-gauge dataset provides good coverage of GB (data for Northern Ireland is absent). Record length varies regionally (Figure 2), with a median of 17 years.

The analyses presented here are based on the study of time-series data for 72,094 rainstorms that contain the *annual maximum* (AM) rainfall intensities for 5-, 10-, 15-, 30-min and 1-, 2-, 3-, 6-, 12- and 24-h durations. A *rainstorm* was defined as a near-continuous spell of rainfall separated from other spells by a sufficiently long dry spell to guarantee statistical independence from other rainfall registered in the same rain gauge. Dry spells are commonly used to separate rainfall events (e.g., De Michele, 2003; Grimaldi et al., 2012; Grimaldi & Serinaldi, 2006; Jun et al., 2021; Koutsoyiannis & Mamassis, 2001; Marra et al., 2020; Molnar et al., 2015; Restrepo-Posada & Eagleson, 1982; Vandenberghe et al., 2010), with most applications relying on an expert criterion to define the length of the dry spell. In our case, the minimum dry spell duration (Figure 2c) was determined using the method of Restrepo-Posada and Eagleson (1982) to avoid defining an arbitrary dry spell duration. A full description of the rainstorm dataset can be found in Villalobos Herrera et al. (submitted).

2.2 | Storm profile methods

Two different methods were used to generate storm profiles from the rainstorm dataset, an overview of both is presented here and more information is available in the Supporting Information (SI).

The original methods used to generate the FSR Summer and Winter profiles, present in Vol. II, Chap. 6 of the FSR (NERC, 1975), were reproduced with some slight modifications to account for differences in event duration (the FSR only studied 24-h events). This method's key characteristic is that it has a centring step where each rainstorm's time series is centred about the shortest duration that contains 50% of the rainfall, D_{50}. The time series of each rainstorm is then divided into concentric hourly windows about the storm centre, T_0, (see Figure 3a, the

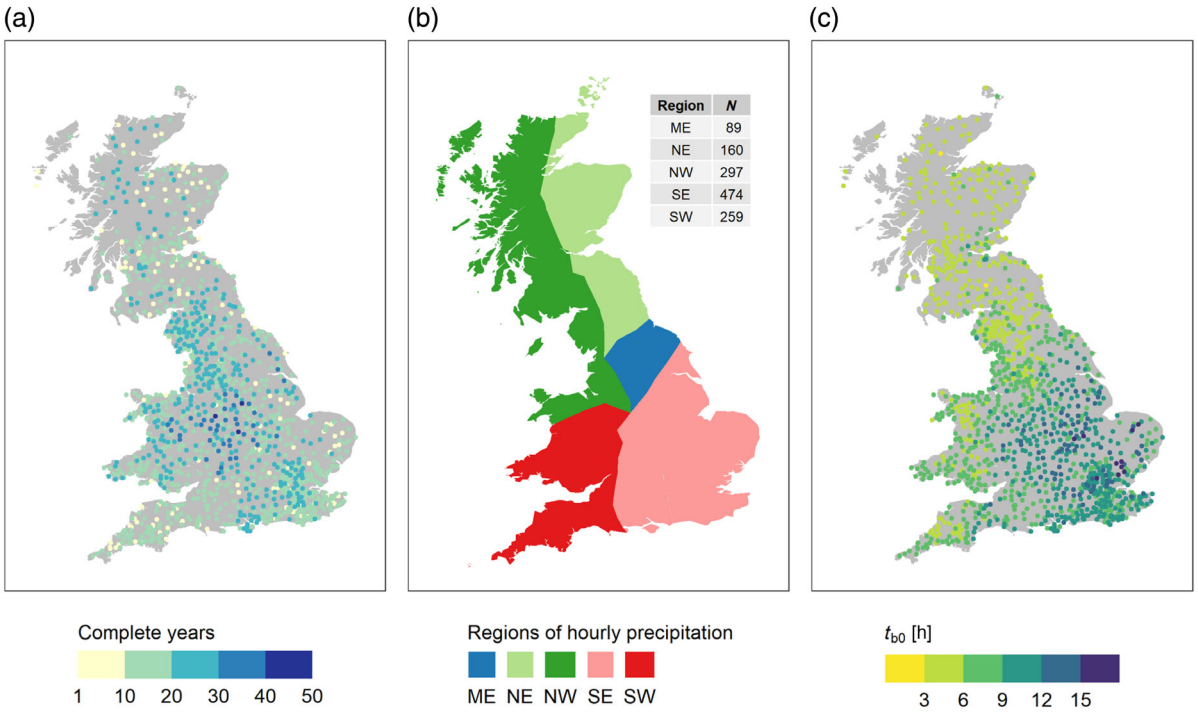

FIGURE 2 (a) Location and length of record of rain gauges with sub-hourly duration, (b) regional classification for hourly rainfall extremes from Darwish et al. (2020) and (c) minimum storm interarrival time, t_{b_0} (in hs), for rain gauges in Great Britain. Inset table in (b) shows the number of rain gauges in each region.

17533318x, 0, Downloaded from https://onlinelibrary.wiley.com/doi/10.1111/jfr3.12958 by Newcastle University, Wiley Online Library on [08/11/2023]. See the Terms and Conditions (https://onlinelibrary.wiley.com/terms-and-conditions) on Wiley Online Library for rules of use; OA articles are governed by the applicable Creative Commons License

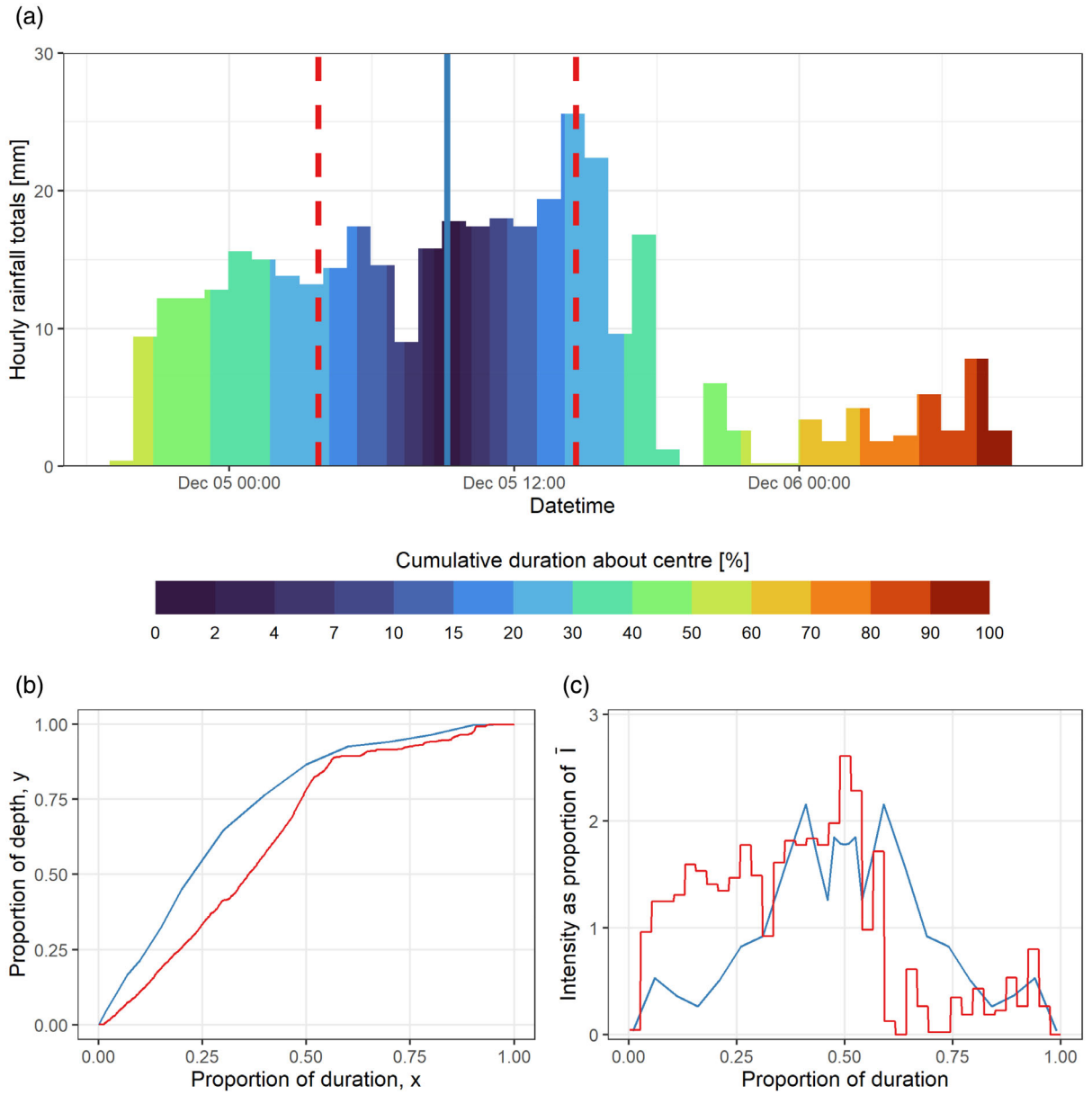

FIGURE 3 For Storm Desmond, as recorded at Honister Pass, December 2015: (a) shortest duration that accumulates 50% of rainfall (D_{50} – red dashed lines), rainstorm centre (T_0 – blue verical line) and centred windows of proportional duration. (b) Cumulative rainfall curve and (c) intensity curve plot according to the centred FSR methodology as adapted for rainstorms of any duration (blue) and without centring (red). FSR profile in (c) is symmetric as per this method's procedure.

centre was assumed to be the middle of the D_{50} window, as implicitly described in the FSR) and the total rainfall at each hour about the centre was calculated as a percentage of the centred 24-h total. Using the same notation as the FEH, this process results in a profile that has *proportion of duration centred on peak* as x, and (cumulative) *proportion of depth* as y (e.g., Figure 1a), while the FSR simply annotates these plots as *percentage of storm duration* against *percentage of storm rainfall*. An example of the profile this produces for a contemporary rainstorm, Storm Desmond in December 2015, can be seen in Figure 3b. The FSR-FEH profiles also use *intensity as a proportion of mean event intensity* as their y-axis variable, it is calculated as $\frac{\Delta y}{\Delta x}$ where Δy is the change in proportional depth that occurs over an Δx interval of proportional duration (see Figure 3b); $\bar{I}$ is the mean event intensity, it has a value of 1 in this scale (e.g., Figures 1a and 3c).

To obtain summary profiles, the FSR ranked events by their *peakedness*, evaluated as the proportion of total event volume that occurred in the middle 5-h of the centred profile- this was modified to the central 20% of

1753318x, 0, Downloaded from https://onlinelibrary.wiley.com/doi/10.1111/jfr3.12958 by Newcastle University, Wiley Online Library on [08/11/2023]. See the Terms and Conditions (https://onlinelibrary.wiley.com/terms-and-conditions) on Wiley Online Library for rules of use; OA articles are governed by the applicable Creative Commons License

event duration for storms that have durations other than 24-h (as 5-h/24-h ~0.2). After ranking, average profiles were calculated: mean y values for each of the centred hourly duration bins x were calculated by averaging across all storms in each quartile of profile peakedness, these average profiles were smoothed by interpolating y values for x values absent in the hourly data. Due to the small number of storms studied in the FSR (80 in summer and 32 in winter), additional profiles were interpolated for the 10, 25, 50, 75, 90 and 95 percentiles of profile peakedness. These interpolated dimensionless profiles (FSR Vol. II, Chap. 6, figs. 6.1 and 6.2) and contemporary example in Figure 3b for comparison) form the basis for the summer and winter profiles shown in Figure 1 (NERC, 1975). This final interpolation was not reproduced in our analysis due to the much larger sample size which allows for a direct estimation of the relevant quantiles.

The second method shares similarities with the FSR method in that it generates dimensionless profiles, however, it avoids the centring step and the use of concentric hourly windows. Instead, profiles are constructed sequentially by calculating each rainstorm's mass curve (its accumulated rainfall depth as a function of event duration) and standardising each curve by total event depth and duration, profiles generated this way are commonly referred to as Huff curves (Huff, 1967) and are used widely (e.g., Dolšak et al., 2016; Kang et al., 2009; Vernieuwe et al., 2015; Wartalska et al., 2020; Yen & Chow, 1983). This method generates dimensionless profiles of percentage of storm duration against percentage of storm rainfall (the same variables the FSR uses; also known as dimensionless rainfall R_d, see Equation S2) but without distorting the profile with the centring step. The dimensionless profiles (e.g., Figure 3b, red line) were calculated at time series resolution of 5- or 15-min. Approximately 38% of the original time series data in our dataset has 15-min resolution, and tip-time data was aggregated to 5-min as this is a factor of 15.

The individual timesteps of dimensionless duration (D_d, see Equation S3) were aggregated into 12 bins of equal length to enable the comparison of events with different durations; any empty bins in short-duration events with fewer than 12 data points were filled in using linear interpolation (~15% of all rainstorms). Twelve bins are used here since that is the number of 5-min intervals that occur in a 1-h event and also sensitivity testing (not shown) of the mean profiles to the number of bins was found to be low.

The dimensionless profiles were classified according to rainstorm duration and volume (depth), region, seasonality, profile shape and profile 'peakedness'. *Rainstorm duration* was classified into four bins that contain an equal number of events, with breaks at 2:10-, 6:45- and 19:25-h (all breaks are notated as HH:MM). From this point onwards, short-duration events are considered as those in the first duration bin (0:15–2:10 h), while long-duration events are those in the last duration bin (19:25 h or greater), all other events are of medium duration. *Rainstorm volume* was classified into three bins based on their empirical frequency within regional and duration bins. For each region and duration combination, events were ranked by volume and classified into percentile-based bins: top 1%, top 10% and all events. This is intended to allow for a simple exploration of whether event magnitude has an impact on rainfall profiles. Regions of *extreme hourly precipitation* (Figure 2b) defined by Darwish et al. (2021) were used to study possible spatial patterns in the data. Both methods consider rainstorms registered during England's bathing season (15 May to 30 September—relevant to water industry since water quality is more closely monitored) as 'summer' events and others as 'winter' events, while the FSR analysis considered May to October as 'summer'.

Profile shape was examined using the timing of the peak rainfall intensity within an event. Rainstorms were separated into five equal-length sections (corresponding to increments of $0.2D_d$ each), and the total R_d for each section was calculated. Rainstorms were then classified according to the section which contained the largest total R_d. Profiles are described as very front-loaded (F2), front-loaded (F1), centred (C), back-loaded (B1) and very back-loaded (B2) according to the section of each event which contains the heaviest rainfall moving from the first to the final $0.2D_d$ section. Finally, *profile peakedness* was evaluated by ranking rainstorms according to the maximum relative intensity within each rainstorm, calculated as the largest step-change in dimensionless cumulative rainfall $\Delta R_d = \max(R_{d,i+1} - R_{d,i})$. Different percentiles of ΔR_d were used in a manner akin to the peakedness rankings used by the FSR method.

The sensitivity of profile shape to these different variables was evaluated by plotting all events grouped within different combinations of categories and visually examining the resulting profile cloud. This allows for a quick comparison between different groups and the different distributions of events within them without relying on mean profiles that may disguise outlying profile shapes or profile variability. Contingency tables (see e.g., Agresti, 2019) and mosaic plots (Hartigan & Hartigan & Kleiner, 1984) were used to complement this visual examination and can be found in the Supporting Information, Tables S2–S4.

Synthetic summary profiles were calculated from the observed dimensionless profiles using three methods. A manual classification method incorporated the findings

1753318x, 0, Downloaded from https://onlinelibrary.wiley.com/doi/10.1111/jfr3.12958 by Newcastle University, Wiley Online Library on [08/11/2023]. See the Terms and Conditions (https://onlinelibrary.wiley.com/terms-and-conditions) on Wiley Online Library for rules of use; OA articles are governed by the applicable Creative Commons License

of the sensitivity analysis to calculate average profiles for events classified by their volume, duration, profile shape and profile peakedness. These results were compared with fully automatic and semi-automatic classification methods. In the fully automatic method, k-means clustering was used to group rainstorms with similar profiles by directly considering the sample of dimensionless profiles (Wu et al., 2006) and the median duration of all rainstorms in each cluster was calculated and added to the profile metadata. In contrast, the semi-automatic method first classified rainstorms by duration after which the k-means algorithm was used.

3 | RESULTS

3.1 | FSR-like profile results

A comparison of the FSR profiles contained in the FEH with new profiles calculated using the same methods, for a much larger number of rainstorms of different durations, challenges some of the original conclusions used in current UK rainfall design methods. Figure 4 shows that event duration has a significant impact on the peakedness of FSR-like profiles at both 50% and 75% percentiles of peakedness. If the artificial assumption of symmetry is accepted, the sharp FSR 50% summer profile included in the FEH is a good match for rainstorms with durations under 6:45-h, especially for winter storms. Note that the original FSR 50% summer profile reaches a maximum intensity of $\sim 3.75\bar{I}$—compared with $\sim 5\bar{I}$ in the FEH version—which is a very good match for the updated 15 min to 2:10-h 50% summer profile. The FSR 75% winter profile—which does not show a difference in peak intensity between FSR and FEH versions—is a better fit for rainstorms with durations over 6:45-h.

Seasonal differences in peak intensity are present in Figure 4, but they are less pronounced than differences between different rainstorm durations. Note that observed summer and winter profiles are only compared to a single FSR profile, as these have different percentiles of peakedness. There is no consistent seasonal pattern regarding peak intensities, as winter profiles for the two shortest duration bins are more peaked than the summer

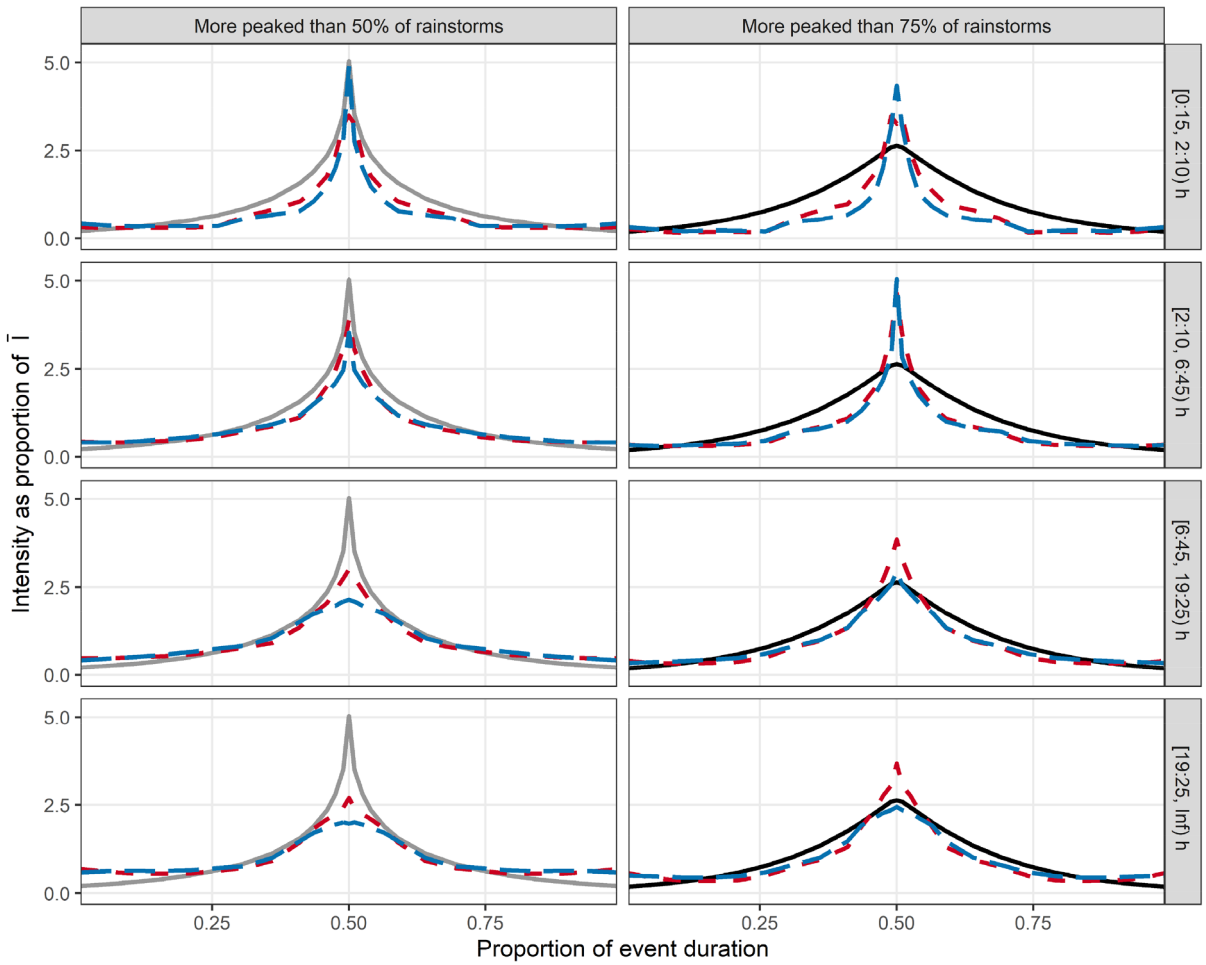

FIGURE 4 FSR-like, 50% most peaked summer profiles (left) and 75% most peaked winter profiles (right) for a set of four increasing duration bins. Reference FSR profiles are shown in grey, new summer and winter profiles are in red and blue, respectively.

1753318x, 0, Downloaded from https://onlinelibrary.wiley.com/doi/10.1111/jfr3.12958 by Newcastle University, Wiley Online Library on [08/11/2023]. See the Terms and Conditions (https://onlinelibrary.wiley.com/terms-and-conditions) on Wiley Online Library for rules of use; OA articles are governed by the applicable Creative Commons License

profiles of the same duration. This is likely an averaging effect, as there are many more extreme summer rainstorms at these durations than there are winter events (14,416 and 3454 rainstorms, respectively). Summer profiles have higher peaks for all other durations. The difference in peak intensity between the observed winter profiles for short-duration events—where the 50% most peaked profile is higher than the 75% profile—represents a limitation in the FSR method's categorization of profile peakedness. The events that have been averaged to form the observed winter 75% profile do concentrate more of their rainfall in the central $0.2D_c$ than those averaged for the 50% profile, but their shape is less sharp; hence, the observed difference in peak intensities.

As expected, the summary FSR profiles are all centred, with their peak intensity occurring in the middle of the storm. This is a result of calculating profiles using bins of proportional duration that are mirrored about the storm's centre. Figure 3c shows that the FSR representation of Storm Desmond underestimates rainfall intensity in the event's first half and at the storm peak, while also overestimating rainfall intensity in the event's back half. This weakness is addressed in the next section using sequential, non-centred and dimensionless profiles.

3.2 | Sensitivity testing of dimensionless profiles

All rainstorms were plotted according to the characteristics that are, a priori, considered to be the most relevant for design: duration, profile shape and frequency (Figure 5), where each characteristic has been classified according to Section 2.2 and the Supporting Information. There is large variation in profile shape at all durations, with little change to the overall spread of profiles among different duration bins. Differences in profile variability for different event duration emerges as events with lower frequencies are considered. Extreme events (top 1% by volume) under 2:10-h show a wide range of shapes, with very steep

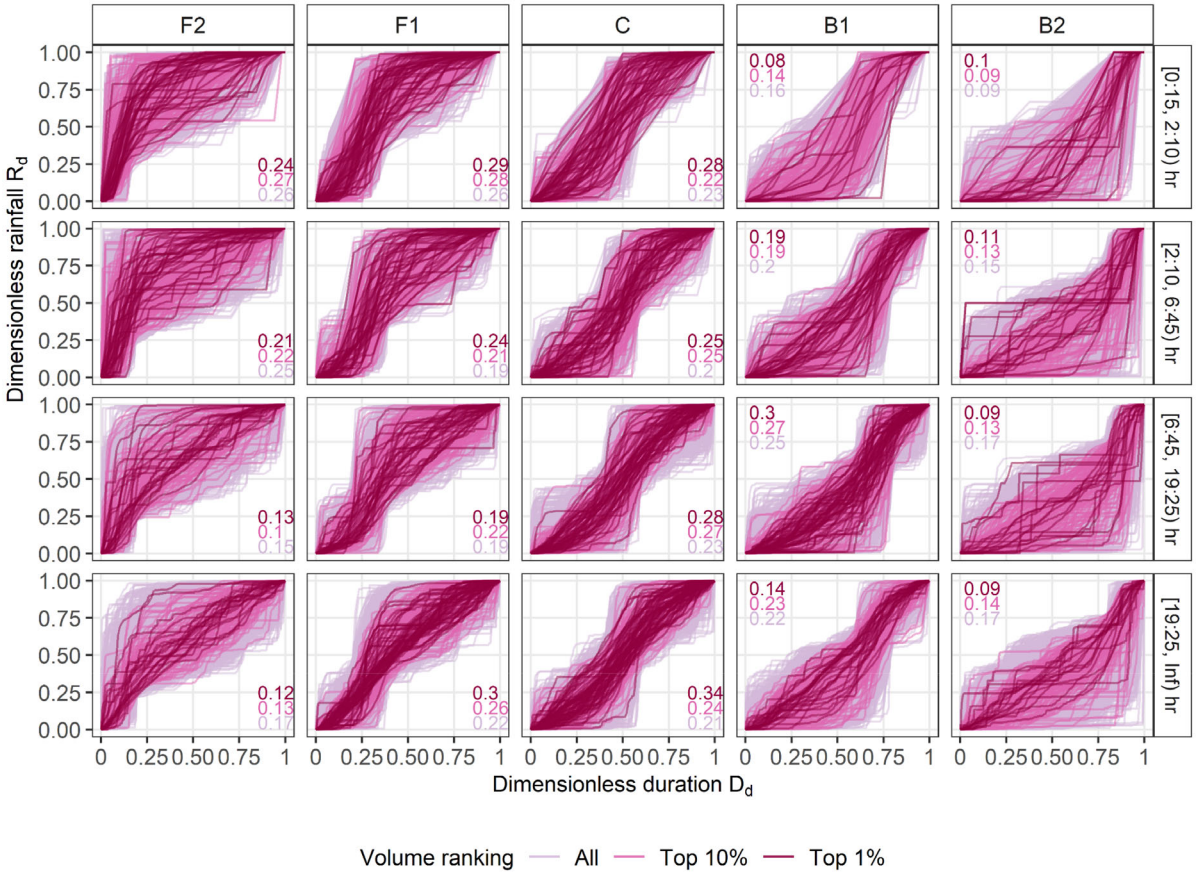

FIGURE 5 Dimensionless profiles for all annual maximum generating rainstorms with at least 3 data points. Profile shape (top panel labels) describes which 0.20 of D_d concentrates the heaviest rainfall, duration bins (right panel labels) contain equal numbers of events, and volume ranking (colour scale) reflects the empirical frequency of events. Rainstorms with larger volumes are plotted on top. Insert text shows the proportional contingency table values for each profile shape—values add up to 1 row-wise (i.e., across each rainstorm duration bin) and are colour coded using the same scale as the volume ranking, with top 1% by volume events first and all events at the bottom. Additional details regarding profile classification can be found in Section 2.

1753318x, 0, Downloaded from https://onlinelibrary.wiley.com/doi/10.1111/jfr3.12958 by Newcastle University, Wiley Online Library on [08/11/2023]. See the Terms and Conditions (https://onlinelibrary.wiley.com/terms-and-conditions) on Wiley Online Library for rules of use; OA articles are governed by the applicable Creative Commons License

profiles found in all shape categories. These steep profiles are not found for extreme events over 19:25-h, where most profiles lie close to the diagonal line representing a near uniform rainfall distribution. This behaviour is expected given the difference in mechanisms that drive GB rainfall extremes of different durations, where heavy long-duration rainstorms are driven by orographic enhancement effects over extended spells of relatively uniform intensity while short-duration storms tend to be convective in nature (Hand et al., 2004; Villalobos Herrera et al., 2022).

The overall frequency of all rainstorms is nearly uniform across different profile shapes (Table 1), with a slight under-representation of B2 profiles. However, for durations under 6:45-h the front-loaded profiles F1 and F2 are more frequent while back-loaded profiles (B1, B2) are less frequent. This pattern is missing in the longest duration bin (>19:25-h), where centred profiles dominate. Intermediate durations show the highest frequencies of C profiles, accompanied with relatively higher frequencies of mildly front- or back-loaded profiles (F1 and B1).

The frequencies of top 10% and top 1% events (by volume) show important deviations from the statistics for all events (see text insets in Figure 5). Short-duration rainstorms show a clear predominance of F1 and F2 profile types among the most extreme events; this increase in front-loaded events is reflected in fewer B1 and B2 events, while C events remain constant. The heaviest long-duration events are concentrated among F1 and C profiles (64% of rainstorms), establishing that centred and mildly front-loaded events dominate the profiles of extreme long-duration rainstorms, even if profile shape differences are small for this duration class. At medium durations, events tend to favour C profile shapes and have few F2 or B2 profiles among the top 1% rainstorms. The full contingency table for Figure 5 can be found in Table S2.

Sensitivity testing of regional and seasonal influences on profile shapes shows that these two variables have little influence in the variation of rainstorm profiles, as a wide range of profile shapes occur in all regions, across all seasons, though they do influence frequency (Tables S3 and S4). First, no seasonal influence on profile shape can be seen in Figure S1 or Figure S2; profiles within all duration and shape bins combinations show similar spread in profile shapes from one region to another. For example, the B2 profiles of 15-min to 2:10-h rainstorms in the NE and SE regions have very similar distributions (Figure S1). Second, Figure S3 shows no difference between the profile distributions of summer and winter rainstorms of different shapes and durations.

The effect of seasonality on the frequency of different duration events is important for GB (Figure 6a); short-duration rainstorms are much more frequent during summer than winter, while long-duration rainstorms are more frequent in winter. This is expected given that warm months are more conducive to producing convective events that produce extreme, intense, rainfall at short durations (under 6-h). Some regional variation exists in the seasonal frequency of long-duration extremes (Figure S4); long-duration rainstorms in westerly regions are more clearly dominated by winter season events than more easterly regions, the latter can have close to a 50/50 split in event frequency between both seasons.

The distribution of profile shapes for rainstorm duration varies across different seasons (Figure 6b,c). Short-duration summer rainstorms are dominated by front-loaded and centred profile shapes. This pattern becomes less clear as rainstorm duration increases and long-duration events slightly favour F1, C and B1 profile shapes (Figure 6b). Differences at a regional level are small (Figure S4).

Winter short-duration events also favour F1, F2 and C profiles, though less so than their summer counterparts, while rainstorms in the two longest duration bins once again favour F1, C and B1 profiles (Figure 6c). Overall, there is evidence that F2 and B2 profile shapes are less frequent among longer-duration events, that is, that longer duration events tend towards more centred profiles. The most noticeable regional variation (Figure S5) is for the SE long-duration events which are nearly evenly distributed among all profile categories; this may be due to the large proportion of summer events within this event duration bin (Figure S4) as summer events are more likely to contain convective components that could skew the event rainfall profile towards F2 or B2 shapes.

TABLE 1 Proportional contingency table for annual maximum generating rainstorms, classified according to their duration and profile shape.

	Profile shape (% per duration bin)				
Duration bin (h)	**F2**	**F1**	**C**	**B1**	**B2**
[0:15, 2:10)	26.4	25.7	22.7	15.8	9.4
[2:10, 6:45)	24.8	19.5	20.4	20.2	15.1
[6:45, 19:25)	15.0	19.4	23.4	24.8	17.4
[19:25, Inf)	16.9	22.2	21.4	22.1	17.4
All	20.6	21.6	22.0	20.8	14.9

Note: Values shown are percentages of all rainstorms in each duration bin.

3.3 | Synthetic profiles for GB rainstorms

3.3.1 | Manual classification

Synthetic profiles were constructed considering event duration, profile shape and peakedness and percentile of

1753318x, 0, Downloaded from https://onlinelibrary.wiley.com/doi/10.1111/jfr3.12958 by Newcastle University, Wiley Online Library on [08/11/2023]. See the Terms and Conditions (https://onlinelibrary.wiley.com/terms-and-conditions) on Wiley Online Library for rules of use; OA articles are governed by the applicable Creative Commons License

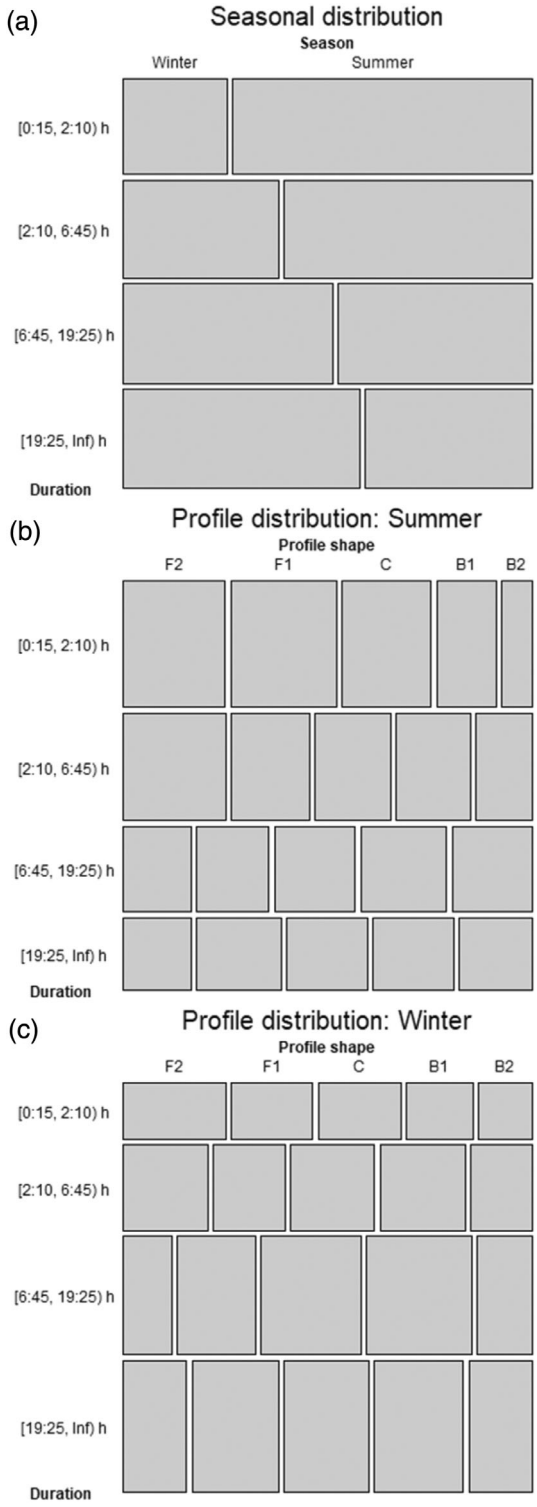

FIGURE 6 Mosaic plots of season and rainstorm duration (a), and of profile shapes for summer (b) and winter (c) rainstorms. All event data is included. Cell edge length along each axis represents relative frequency, and cell area indicates overall proportion relative to all events in each season.

volume (as proxy for frequency) as the most relevant rainstorm characteristics for design. Duration is used instead of seasonality as their effects can be confounded (as in the FSR); however, rainstorm duration can be related to rainfall generating mechanisms such as convection—for short durations—which while more frequent in summer, may also occur in winter. In addition, storm duration is an important design parameter as it relates to the time of concentration concept often used in rainfall design methods.

Figure 7 shows the mean profiles for rainstorms in the top 10% of volume, classified according to their profile shape, peakedness and duration. Large events are used as these are most likely to have significant impacts and this includes the most severe (top 1%) events while still providing a large rainstorm sample. The most peaked mean profile corresponds to short-duration, F2 profile rainstorms that have ΔR_d higher than 90% of other events, with a peak of $7.32\bar{I}$ and virtually all rainfall occurring within the first 1/3 of the event. F2 and B2 profiles show the highest intensities in all duration bins; recall however that rainstorms with these profile types become rarer as event duration and volume increase (Figure 5 inset text). The smaller sample size available for the $90\%\Delta R_d$ rainstorms—especially in long-duration F2 and B2 profile shapes—is also reflected as variability or jaggedness in the corresponding mean profiles.

The peak intensities of long-duration rainstorm profiles are lower than their counterparts for shorter durations: this is most noticeable in F2 and B2 profiles (Figure 7). Smaller changes are seen across different durations for F1, C and B1 profiles, with peak intensities staying below $3.5\bar{I}$ for the two longer duration bins, and below $4\bar{I}$ in all but the most intense B1 profiles for the two shorter duration bins.

When compared to the summer 50% most peaked FSR profile, 17 mean profiles (out of 100 total profiles in Figure 7) exceed the original peak intensity of $3.75\bar{I}$ (Figure 1), 4 of these mean profiles also exceed the higher $5\bar{I}$ peak intensity shown in the FEH version of the profile (Figure 1). The FEH version of the profiles is more conservative due to its higher peak intensity; however, none of the centred profiles reach this peak intensity. Overall, F2 profiles are those most prone to exceeding the FEH 50% summer profile's peak intensity (Figure 7).

The winter 75% FSR profile which peaks at $\sim 2.5\bar{I}$ is exceeded by 58 of all mean profiles shown in Figure 7. More importantly, all $90\%\Delta R_d$ profiles for rainstorms with durations over 6:45 meet or exceed this intensity and front-loaded or back-loaded profiles with lower percentiles of ΔR_d frequently exceed this intensity.

3.3.2 | Automatic classification results

The k-means clustering algorithm, executed on profiles from all rainstorm durations, produces results that are

17533180x, 0, Downloaded from https://onlinelibrary.wiley.com/doi/10.1111/jfr3.12958 by Newcastle University, Wiley Online Library on [08/11/2023]. See the Terms and Conditions (https://onlinelibrary.wiley.com/terms-and-conditions) on Wiley Online Library for rules of use; OA articles are governed by the applicable Creative Commons License

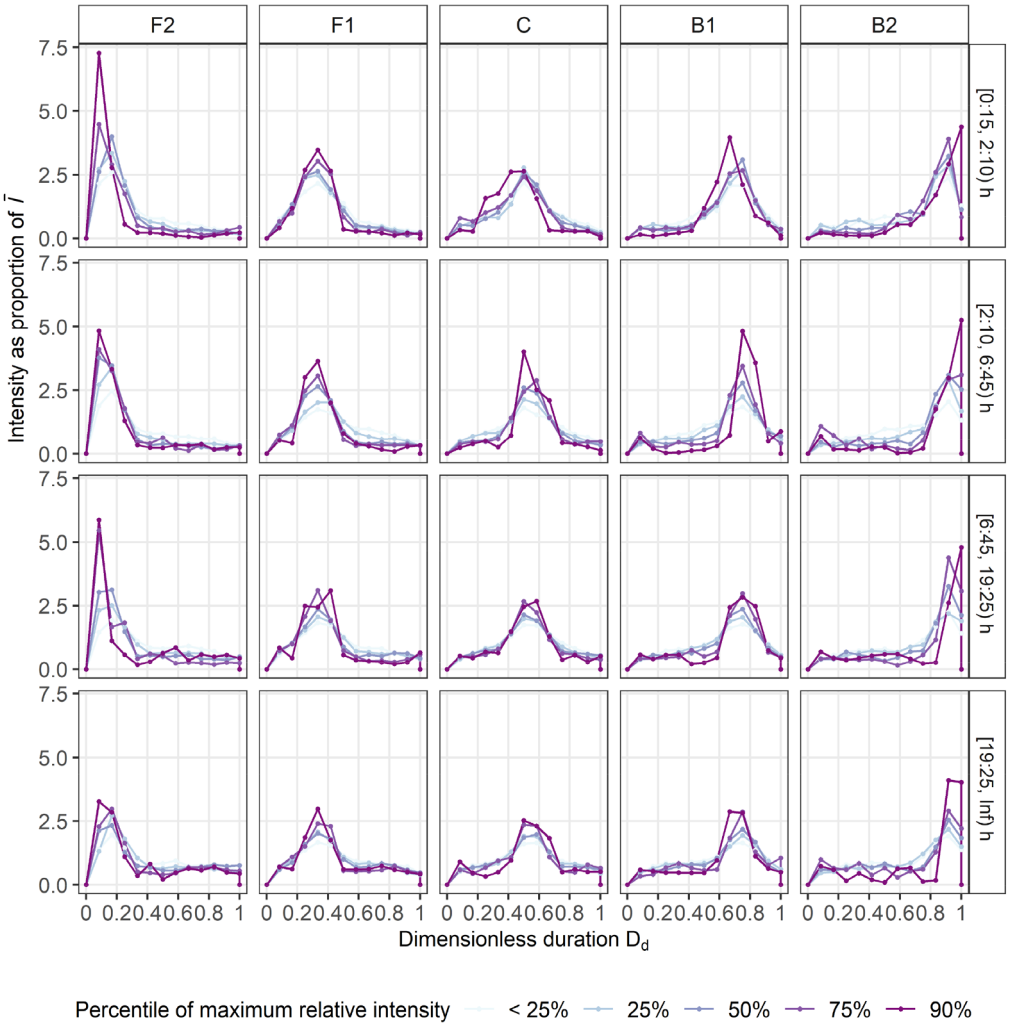

FIGURE 7 Mean intensity synthetic profiles for different percentiles of maximum relative intensity, with rainstorms classified according to their profile shape and duration. The X% profile is the mean of all events that have a higher maximum relative intensity than X% of other events in the same duration and shape bin, for example, the F2 90% profile is averaged from all events that exceed the 90th percentile of maximum relative intensity for all F2 events. Only the top 10% rainstorms by volume were used.

coherent with the manual classification (Figure 8 and Figure S6). The five synthetic profiles generated by using five clusters (top row) matches the manual classification of events into five profile shapes, this confirms the validity of using of these shape categories as indicative of differences between event profiles. Increasing the number of clusters highlights differences between rainstorms within each profile shape category and ensures more profile variability is represented in the resulting profiles (Figure S6), however, near duplicate profiles are observed once more than 25 clusters are used. This behaviour was confirmed by plotting the within-groups sum of squares (WSS) metric against number of clusters, this shows an elbow around 5–10 clusters and a rapid decrease in WSS variation past 25 clusters (Figure S7). Different number of profiles appear in each shape category as the number of clusters is increased, for example, when using 25 clusters only 3 of those are of shape B1, while shapes F2 and F1 have 6 clusters (profiles) each. Further, as cluster number increases the number of clusters associated with rainstorms of under 6-h increases more than those of longer-duration events, suggesting that short-duration rainstorms have greater variability in profile shape than long events. Differences in profile shape frequency relative to duration (discussed in detail in Section 3.2) can be seen throughout, with darker colours among less steep profiles, while the steepest F1 and F2 profiles have light colours reflecting median rainstorm durations under 3 h within these clusters. The next most peaked profiles tend to come from clusters with median durations between 3 and 6 h.

A mixed classification scheme, where 15 clusters were automatically identified using the k-means algorithm at each manually chosen rainstorm duration bin (Figure 9) also shows similar results to those seen during manual classification of events (Figure 7). There is a clear decrease in peak intensities in the F2 profiles with increases in duration; this not observed in the B2 profiles. The most peaked F1, C and B1 profiles are found in the shortest duration bin, and overall, these profiles show lower peak intensities than F2 and B2.

The mixed classification scheme shows a greater variation in profile shape among rainstorms with durations

1753318x, 0, Downloaded from https://onlinelibrary.wiley.com/doi/10.1111/jfr3.12958 by Newcastle University, Wiley Online Library on [08/11/2023]. See the Terms and Conditions (https://onlinelibrary.wiley.com/terms-and-conditions) on Wiley Online Library for rules of use; OA articles are governed by the applicable Creative Commons License

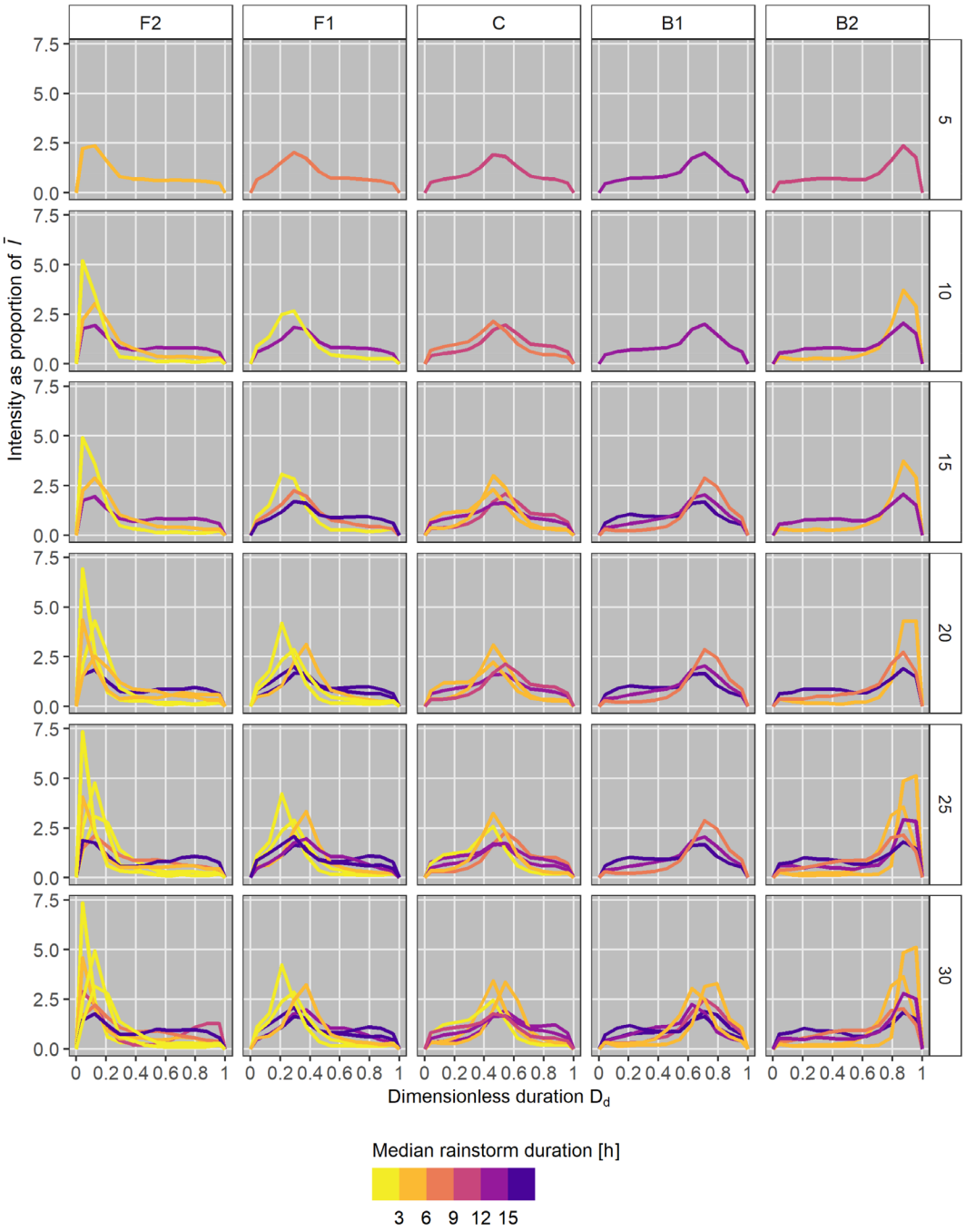

FIGURE 8 Mean intensity profiles for different clusters of events as identified by a k-means algorithm from all top 10% rainstorms by volume, shaded according to the median rainstorm duration of each cluster. Profiles are classified by shape after clustering, and the number of clusters is indicated on the right panel labels.

under 6:45 than for longer duration ones, this is especially true for F2 and F1 profiles. In all duration bins for rainstorms over 2:10-h long show there is very little variation in F1, C and B1 profiles. It is likely that aggregation processes are at play here, as any short-duration variations in rainfall intensities within long-duration events are masked out using 12 D_d bins (e.g., consider that a 24-h event would be represented by 12 2-h intervals, masking any variation in intensity below that duration). This effect could be removed by varying the number of D_d bins with duration, this was not done here as it was considered more important to use a uniform method for rainstorms of all durations.

There are remarkable coincidences between all three classification methods. Chief among these is the trend towards lower peak relative intensities as duration increases, and the extraordinarily high peak intensities of short-duration F2 and F1 profiles.

1753318x, 0, Downloaded from https://onlinelibrary.wiley.com/doi/10.1111/jfr3.12958 by Newcastle University, Wiley Online Library on [08/11/2023]. See the Terms and Conditions (https://onlinelibrary.wiley.com/terms-and-conditions) on Wiley Online Library for rules of use; OA articles are governed by the applicable Creative Commons License

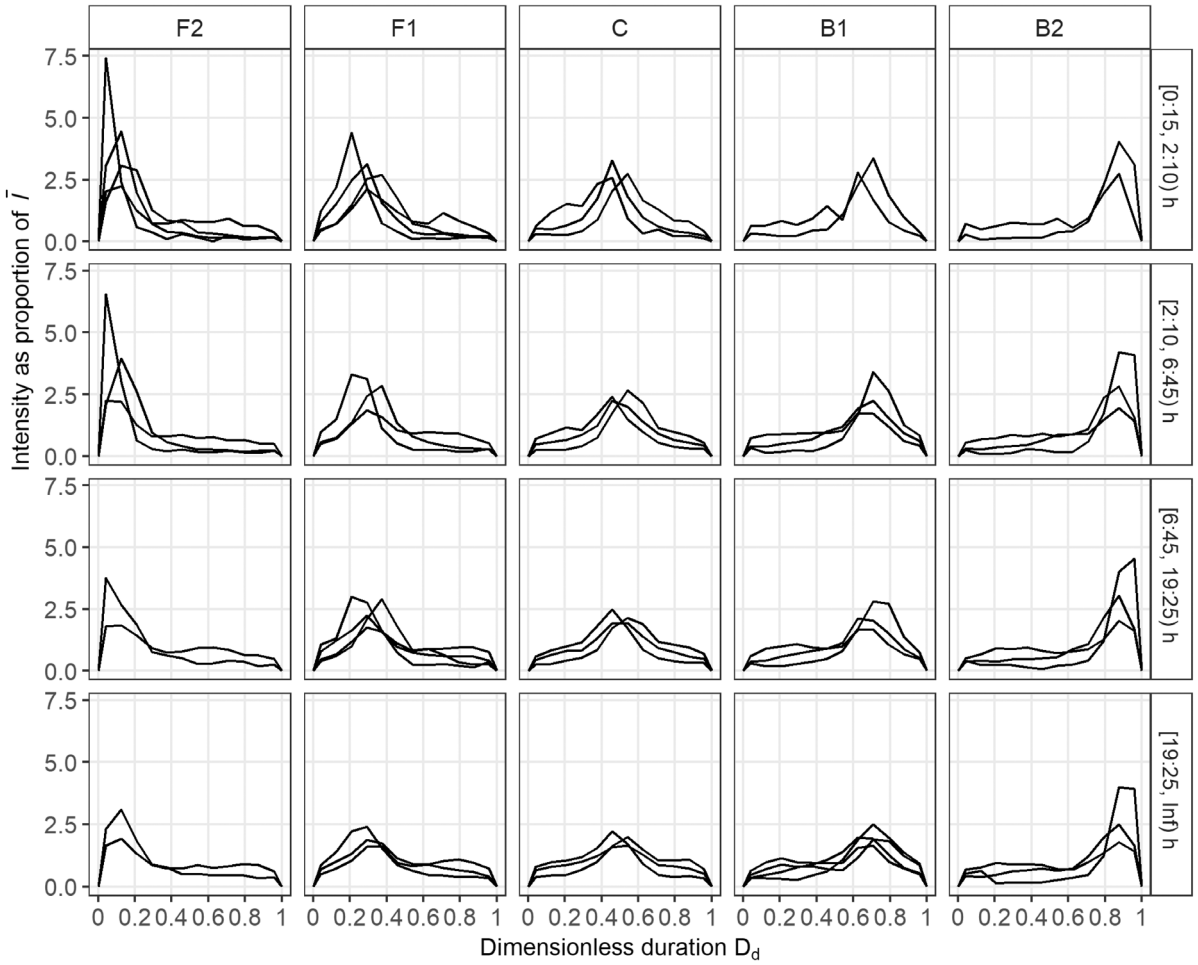

FIGURE 9 Mean intensity profiles for 15 clusters at each duration category generated using a k-means algorithm, for all top 10% rainstorms by volume. Profiles are classified by shape after clustering.

4 | DISCUSSION

We have applied the FSR methodology to a large, modern sub-hourly rainfall dataset for GB, revealing limitations in the methods and conclusions of this seminal work on storm profiles. Firstly, the FSR method produces rainstorm profiles centred about the moment of peak rainfall intensity by averaging over proportional duration bins that span both sides of the rainstorm's centre. This removes information on the timing of the storm's peak intensity (i.e., whether the rainstorm is front-loaded, back-loaded or centred) as peak intensity is always moved to the centre, also smoothing out some temporal variation as rainfall at either end of the storm centre is averaged together (Figure 3). Subsequent averaging (across multiple rainstorms) then yields uniformly centred profiles (Figure 4) which under-represent the variation found in dimensionless rainstorm profiles that are not centred (Figure 5). In addition, our results contradict the FSR's claims on the universal applicability of their profiles to different duration rainstorms. We find that longer-duration events have lower peak intensities and vice versa (Figure 4). Further, our larger dataset indicates that rainfall profiles are not seasonally dependent, refuting the FSR recommendation that design rainfall profiles should vary between 'summer' and 'winter'.

Our study confirms the immense variation in rainstorm profile shapes in GB (Figure 5) also found in other regions such as Australia (J. Ball et al., 2019) and the USA (Bonnin et al., 2011). A significant proportion of these events are not centred; especially at durations under 6:45-h, where over half of rainstorms are front-loaded. This variation over the event decreases among the biggest (by volume) long-duration rainstorms, producing more centred F1 and C shapes (Figures 5–9). Our sensitivity testing of different rainstorm attributes shows that few variables truly modify profile shape. Rainstorm duration is the most important variable (Figures 4, 5 and S1–S3), and longer duration events tend to have less variable profiles than shorter rainstorms. This is expected given that different rain-generating mechanisms drive

1753318x, 0, Downloaded from https://onlinelibrary.wiley.com/doi/10.1111/jfr3.12958 by Newcastle University, Wiley Online Library on [08/11/2023]. See the Terms and Conditions (https://onlinelibrary.wiley.com/terms-and-conditions) on Wiley Online Library for rules of use; OA articles are governed by the applicable Creative Commons License

rainfall extremes at different durations (Darwish et al., 2018; Hulme & Barrow, 1997, Villalobos Herrera, et al., submitted). Profile shape is also closely related to rainstorm magnitude (Figure 5), especially for long-duration events.

We find that seasonal and regional variations in profile shape are the result of changes to the frequency of different duration events. Both short-duration and long-duration events have similar profile range across all seasons and regions (Figures S1–S3). However, since long/short duration events are more frequent in winter/summer, front-loaded events are more frequent in the summer while centred profile shapes dominate winter (Figure S5).

The three methods we use to derive synthetic profiles for GB rainstorms produce consistent results (Figures 7–9), although the unsupervised classification methods are more objective as fewer assumptions are made on profile classification. K-means classification with no duration binning is the least biased and most parsimonious method (as cluster number is the main user-defined variable, with 15–25 clusters showing a good balance between profile variability and avoiding duplication), and once post-processed it provides an easy-to-explain and intuitive classification. The duration-binned k-means classification is a good intermediate, which combines a key hydrological variable (event duration) with an unbiased classification method.

Methodologically, an advantage of manual classification over a procedure such as k-means clustering is reproducibility, as the latter, automatic procedure relies on a random selection of cluster starting points which may vary between runs (a fixed seed has been used here to mitigate this). Meanwhile, assumptions made in manual classification methods could significantly affect results. Sensitivity tests demonstrate that using different duration bins, different percentiles of ΔR_d and different numbers of profile shapes—for example, using three shapes rather than five—will modify the resulting mean profile shapes, (e.g., Figure S8). The less biased results provided by a clustering algorithm may therefore be preferred. We find that short-duration rainstorms with the most front-loaded (F2) profiles reach the highest peak intensities, followed by the most back-loaded (B2) profiles. More centred F1, C and B1 profiles have similar peak intensities, with some evidence of a decrease in peak intensities for longer-duration rainstorms (Figure 8). Compared to the FSR profiles, a number of F2 and B2 profiles—generated by all three methods—reach very high relative intensities that exceed the 50% summer profile in current use for urban catchment design in the UK, while most synthetic profiles exceed the 75% winter profile used for rural catchments.

5 | CONCLUSIONS AND RECOMMENDATIONS

In current UK guidance for use of design storms, the choice of FSR profile is based on catchment characteristics: the FEH recommends that the 75% winter profile be used in rural catchments, with the 50% summer profile recommended for urban catchments (Faulkner, 1999). EA flood estimation guidance provides urban extent limits to apply this recommendation (Environment Agency, 2022), while SEPA guidance recommends use of the summer profile for small catchments, urban catchments and for all surface water flooding applications (SEPA, 2019). These recommendations make no distinction regarding storm duration (except for some reservoir safety applications), following FSR guidance that the FSR profiles may be used for storms of any duration 'up to several days' (Faulkner, 1999; NERC, 1975). Our analysis provides new insight, contradicting some of the FSR recommendations, and revealing that storm duration is key to determining profile shape. We thus recommend that this critical factor is considered when selecting a storm profile for use in hydrological simulations. Our study indicates that failing to consider the interaction between event duration (and the different profile shapes associated with it) and catchment response times may lead to under- or over-estimation of flood extents, peak flows and runoff volumes.

Our results show an incredible range of variation in event profiles across the UK; the use of a single, centred, FSR profile fails to represent this observed profile variability. Since different rainfall profiles generate differing hydrological responses, evaluating the impact of different plausible profiles on catchments, urban areas, sewer networks and other infrastructure is and will be key to ensuring robust designs, and we would recommend that a broad selection are used. However, the use of a single profile or profile family may continue to be useful for applications where the assumptions behind a single profile are justified, while complex or critical infrastructure may be modelled using more involved modelling approaches such as profile ensemble testing or Monte Carlo simulation (J. Ball et al., 2019).

All three summary profile methods consistently generate profiles with peak intensities that exceed those recommended in the FSR 50% summer profile. The use of the FSR profiles in urban or fast-response catchments may thus result in infrastructure designs that are underprepared to cope with observed high-intensity rainfall events and flood risk analyses which underestimate flood depths and velocities. However, the long-duration events that are more relevant to rural catchment applications show peak intensities close to those of the 75% winter

1753318x, 0, Downloaded from https://onlinelibrary.wiley.com/doi/10.1111/jfr3.12958 by Newcastle University, Wiley Online Library on [08/11/2023]. See the Terms and Conditions (https://onlinelibrary.wiley.com/terms-and-conditions) on Wiley Online Library for rules of use; OA articles are governed by the applicable Creative Commons License

profile; thus, differences in the timing of peak intensities are more likely to be relevant uncertainties here.

Most hydrological design methods in which the FSR profiles are used are set up in a way that adjusts the composition of the design event (storm profile, return period, duration and initial catchment wetness) so that the resulting flood hydrograph has a peak flow consistent with the results of flood frequency analysis. This is still the case for the current version of the fluvial design method, the Revitalised Flood Hydrograph model (Wallingford HydroSolutions, 2019), which should provide some reassurance over concerns about under-design. However, there are benefits to having more realistic ingredients to the design event. One is the avoidance of the need to over-compensate one component to make up for the shortcomings of another (such as unrealistically flat design profiles). Another benefit stems from the fact that peak flows are not the only influence on flood hazard. The choice of rainfall profile affects the shape of the flood hydrograph, which interacts with the physical characteristics of the river or drainage system, for example, with early flow peaks filling up storage areas.

A similar adjustment process was followed to develop the Wallingford Procedure for urban drainage design (Kellagher, 1981). However, current versions of urban drainage design models are not set up to preserve the relationship between rainfall and peak flow return periods (Dale et al., 2022). There is no guarantee that any such probabilistic relationship will be maintained if any of the components of the design event are changed; for example, if different storm profiles are used. For this reason, any change in profiles needs to be accompanied by a recalibration of the design inputs; something which is needed, in any case, for drainage design methods.

It is evident that the FSR profiles need replacement. They fail to represent the different observed profile shapes and their key assertion that profile shape is consistent across event durations is false. Rainstorm duration and magnitude are the key variables that constrain profile shapes in GB; therefore, any replacement of the FSR profiles should consider these variables within their analysis. Some consideration should also be given to plausible future changes in event profile shape, as evidence suggests profiles are changing to become more peaked with global warming (Fowler et al., 2021; Wasko et al., 2021; Wasko & Sharma, 2015).

Work carried out as part of a study for UK Water Industry Research (UKWIR) tested the impacts of using different rainfall profiles (the FSR profiles and preliminary, less-intense versions of the profiles shown in Figure 7) on sewer network models, with results that show significant variability between different profiles and network models (Dale et al., 2022). This case study is only one among the wide range of applications that use the FSR profiles, and it highlights the need to evaluate the effect of the updated, more intense rainstorm profiles presented here, on natural and artificial drainage systems.

There are many alternatives for FSR replacement profiles. Here, three methods for producing synthetic, design profiles were explored, with satisfactory and consistent results. There are other options, such as observed event ensembles or stochastic methods of profile generation, which were not explored in detail here, but that are plausible replacements for the FSR. There is now a need for scientists, practitioners and regulators to discuss the best course of action towards more robust UK rainfall design guidance.

ACKNOWLEDGEMENTS

Roberto Villalobos Herrera acknowledges funding from the Universidad de Costa Rica and the School of Engineering of Newcastle University. Hayley J. Fowler is funded by the FUTURE-STORMS (NE/R01079X/1), FUTURE-DRAINAGE (NE/S017348/1) and STORMY-WEATHER (NE/V004166/1) projects. Stephen Blenkinsop is funded by the FUTURE-STORMS project. Murray Dale and Duncan Faulkner were funded by UKWIR project 22/CL/10/19: Climate Change Rainfall for use in Sewerage Design—Design Storm Profiles, Antecedent Conditions, RedUp Tool Update and Seasonality Impacts. Part of this work was funded by the European Research Council Grant, INTENSE (ERC-2013-CoG-617329).

DATA AVAILABILITY STATEMENT

The original data are in the public domain and available for download from the providers instructions to download EA data can be found at https://environment.data.gov.uk/flood-monitoring/doc/rainfall, instructions to download NRW data can be found at https://api-portal.naturalresources.wales/docs/services/open-data-river-level-rainfall-and-sea-data-api/operations/historicaldataforstationparameter, and instructions to download SEPA data can be found at https://www2.sepa.org.uk/rainfall. QC associated scripts are available at https://github.com/nclwater/intense-qc and https://github.com/nclwater/SubHourlyQC.

ORCID

Roberto Villalobos Herrera https://orcid.org/0000-0002-0853-2285
Duncan Faulkner https://orcid.org/0000-0002-7471-7819

REFERENCES

Agresti, A. (2019). An introduction to categorical data analysis. In *Wiley series in probability and statistics* (3rd ed.). John Wiley and Sons.

1753318x, 0, Downloaded from https://onlinelibrary.wiley.com/doi/10.1111/jfr3.12958 by Newcastle University, Wiley Online Library on [08/11/2023]. See the Terms and Conditions (https://onlinelibrary.wiley.com/terms-and-conditions) on Wiley Online Library for rules of use; OA articles are governed by the applicable Creative Commons License

Ball, J., Babister, M., Nathan, R., Weeks, W., Weinmann, E., Retallick, M., & Testoni, I. (2019). *Australian rainfall and runoff: A guide to flood estimation*. Geoscience Australia http://arr.ga.gov.au/

Ball, J. E. (1994). The influence of temporal patterns on surface runoff hydrographs. *Journal of Hydrology*, *158*(3–4), 64–69.

Bonnin, G. M., Martin, D., Lin, B., Parzybok, T., Yekta, M., & Riley, D. (2011). *NOAA Atlas 14—Precipitation-Frequency Atlas of the United States* (Vol. 1). https://www.weather.gov/media/owp/oh/hdsc/docs/Atlas14_Volume1.pdf

Butler, D., & Davies, J. W. (2011). *Urban drainage* (3rd ed.). Taylor & Francis.

Chow, V. T., Maidment, D. R., & Mays, L. W. (1988). *Applied hydrology*. McGraw-Hill.

CIWEM. (2016). *Rainfall modelling guide 2016*. London.

Cordery, I., Pilgrim, D. H., & Rowbottom, I. A. (1983). Time patterns of rainfall for estimating design floods on a frequency basis. *Water Science and Technology*, *16*(8/9), 155–165.

Dale, M., Faulkner, D., Fowler, H. J., Gill, E., Shelton, K., Titterington, J., & Villalobos Herrera, R. (2022). 22/CL/10/19—Climate Change Rainfall for use in Sewerage Design—Design Storm Profiles, Antecedent Conditions, RedUp Tool Update and Seasonality Impacts (Technical Report). https://ukwir.org/water-research-reports-publications-viewer/f6d9cb31-0108-4535-9b09-cf0d8c1bb801

Darwish, M. M., Fowler, H. J., Blenkinsop, S., & Tye, M. R. (2018). A regional frequency analysis of UK sub-daily extreme precipitation and assessment of their seasonality. *International Journal of Climatology*, *38*(13), 4758–4776. https://doi.org/10.1002/joc.5694

Darwish, M. M., Tye, M. R., Prein, A. F., Fowler, H. J., Blenkinsop, S., Dale, M., & Faulkner, D. (2021). New hourly extreme precipitation regions and regional annual probability estimates for the UK. *International Journal of Climatology*, *41*(1), 582–600. https://doi.org/10.1002/joc.6639

De Michele, C. (2003). A generalized pareto intensity-duration model of storm rainfall exploiting 2-Copulas. *Journal of Geophysical Research*, *108*(D2), 4067. https://doi.org/10.1029/2002JD002534

Dolšak, D., Bezak, N., & Šraj, M. (2016). Temporal characteristics of rainfall events under three climate types in Slovenia. *Journal of Hydrology*, *541*, 1395–1405. https://doi.org/10.1016/j.jhydrol.2016.08.047

Environment Agency. (2022). Flood Estimation Guidelines. Instruction LIT 11832 (Issue 197).

Faulkner, D. (1999). *Rainfall frequency estimation, Volume 2 of the flood estimation handbook*. Centre for Ecology and Hydrology.

Fowler, H. J., Ali, H., Allan, R., Ban, N., Barbero, R., Berg, P., Blekinsop, S., Cabi, N., Chan, S., Dale, M., Dunn, R., Ekstrom, M., Evans, J., Fosser, G., Golding, B., Guerreiro, S., Hegerl, G., Kahraman, A., Kendon, E., … Whitford, A. (2021). Towards advancing scientific knowledge of climate change impacts on short-duration rainfall extremes. *Philosophical Transactions A: Mathematical, Physical and Engineering Sciences*, *379*(2195), 1–22. https://doi.org/10.1098/rsta.2019.0542

Grimaldi, S., Petroselli, A., & Serinaldi, F. (2012). Design hydrograph estimation in small and ungauged watersheds: Continuous simulation method versus event-based approach. *Hydrological Processes*, *26*(20), 3124–3134. https://doi.org/10.1002/hyp.8384

Grimaldi, S., & Serinaldi, F. (2006). Design hyetograph analysis with 3-copula function. *Hydrological Sciences Journal, 51*(2), 3124–3134. https://doi.org/10.1623/hysj.51.2.223

Hand, W. H., Fox, N. I., & Collier, C. G. (2004). A study of twentieth-century extreme rainfall events in the United Kingdom with implications for forecasting. *Meteorological Applications*, *11*(1), 15–31. https://doi.org/10.1017/S1350482703001117

Hartigan, J. A., & Kleiner, B. (1984). A mosaic of television ratings. *The American Statistician*, *38*(1), 32–35. https://www.jstor.org/stable/2683556

Hettiarachchi, S., Wasko, C., & Sharma, A. (2018). Increase in flood risk resulting from climate change in a developed urban watershed—The role of storm temporal patterns. *Hydrology and Earth System Sciences*, *22*(3), 2041–2056. https://doi.org/10.5194/hess-22-2041-2018

Huff, F. (1967). Time distribution rainfall in heavy storms. *Water Resources Research*, *3*(4), 1007–1019. https://doi.org/10.1029/WR003i004p01007

Hulme, M., & Barrow, E. (Eds.). (1997). *Climates of the British Isles: Present, past, and future*. Routledge.

Institute of Hydrology. (1999). *Flood estimation handbook* (Vol. 1–5). Institute of Hydrology.

Institution of Civil Engineers (ICE). (2015). *Floods and reservoir safety* (4th ed.). ICE Publishing. https://doi.org/10.1680/frs.60067

Jun, C., Qin, X., Chen, M., & Seo, H. (2021). Investigating event-based temporal patterns of design rainfall in a tropical region. *Hydrological Sciences Journal*, *66*(13), 1986–1996. https://doi.org/10.1080/02626667.2021.1967958

Kang, M. S., Koo, J. H., Chun, J. A., Her, Y. G., Park, S. W., & Yoo, K. (2009). Design of drainage culverts considering critical storm duration. *Biosystems Engineering*, *104*(3), 425–434. https://doi.org/10.1016/j.biosystemseng.2009.07.004

Kellagher, R. (1981). *The Wallingford procedure—For design and analysis of urban storm drainage*. HR Wallingford. https://eprints.hrwallingford.com/37/

Koutsoyiannis, D., & Mamassis, N. (2001). On the representation of hyetograph characteristics by stochastic rainfall models. *Journal of Hydrology*, *251*(1–2), 65–87. https://doi.org/10.1016/S0022-1694(01)00441-3

Lambourne, J. J., & Stephenson, D. (1987). Model study of the effect of temporal storm distributions on peak discharges and volumes. *Hydrological Sciences Journal*, *32*(2), 215–226. https://doi.org/10.1080/02626668709491179

Lewis, E., Pritchard, D., Villalobos-Herrera, R., Blenkinsop, S., McClean, F., Guerreiro, S., Schneider, U., Becker, A., Finger, P., Meyer-Christoffer, A., Rustemeier, E., & Fowler, H. J. (2021). Quality control of a global hourly rainfall dataset. *Environmental Modelling & Software*, *144*, 105169. https://doi.org/10.1016/j.envsoft.2021.105169

Marra, F., Borga, M., & Morin, E. (2020). A unified framework for extreme subdaily precipitation frequency analyses based on ordinary events. *Geophysical Research Letters*, *47*(18), 1–8. https://doi.org/10.1029/2020GL090209

Molnar, P., Fatichi, S., Gaál, L., Szolgay, J., & Burlando, P. (2015). Storm type effects on super Clausius-Clapeyron scaling of intense rainstorm properties with air temperature. *Hydrology and Earth System Sciences*, *19*(4), 1753–1766. https://doi.org/10.5194/hess-19-1753-2015

1753318x, 0, Downloaded from https://onlinelibrary.wiley.com/doi/10.1111/jfr3.12958 by Newcastle University, Wiley Online Library on [08/11/2023]. See the Terms and Conditions (https://onlinelibrary.wiley.com/terms-and-conditions) on Wiley Online Library for rules of use; OA articles are governed by the applicable Creative Commons License

Müller, T., Schütze, M., & Bárdossy, A. (2017). Temporal asymmetry in precipitation time series and its influence on flow simulations in combined sewer systems. *Advances in Water Resources*, *107*, 56–64. https://doi.org/10.1016/j.advwatres.2017.06.010

NERC. (1975). *Flood studies report* (Vol. 2). Meteorological Studies.

Nguyen, V. T. V., Desramaut, N., & Nguyen, T. D. (2010). Optimal rainfall temporal patterns for urban drainage design in the context of climate change. *Water Science and Technology*, *62*(5), 1170–1176. https://doi.org/10.2166/wst.2010.295

Pochwat, K., Słyś, D., & Kordana, S. (2017). The temporal variability of a rainfall synthetic hyetograph for the dimensioning of stormwater retention tanks in small urban catchments. *Journal of Hydrology*, *549*, 501–511. https://doi.org/10.1016/j.jhydrol.2017.04.026

Restrepo-Posada, P. J., & Eagleson, P. S. (1982). Identification of independent rainstorms. *Journal of Hydrology*, *55*(1–4), 303–319. https://doi.org/10.1016/0022-1694(82)90136-6

SEPA. (2019). Technical Flood Risk Guidance for Stakeholders-SEPA Requirements for Undertaking a Flood Risk Assessment (Issue 12). https://www.sepa.org.uk/media/162602/ss-nfr-p-002-technical-flood-risk-guidance-for-stakeholders.pdf

United States Department of Agriculture. (1986). Urban hydrology for small watersheds. In *Soil conservation* (Issue Technical Release 55 (TR-55)). http://scholar.google.com/scholar?hl=en&btnG=Search&q=intitle:Urban+Hydrology+for+Small+watersheds#1

Vandenberghe, S., Verhoest, N. E. C., Buyse, E., & De Baets, B. (2010). A stochastic design rainfall generator based on copulas and mass curves. *Hydrology and Earth System Sciences*, *14*(12), 2429–2442. https://doi.org/10.5194/hess-14-2429-2010

Vernieuwe, H., Vandenberghe, S., De Baets, B., & Verhoest, N. E. C. (2015). A continuous rainfall model based on vine copulas. *Hydrology and Earth System Sciences*, *19*(6), 2685–2699. https://doi.org/10.5194/hess-19-2685-2015

Villalobos Herrera, R., Blenkinsop, S., Guerreiro, S. B., O'Hara, T., & Fowler, H. J. (2022). Sub-hourly resolution quality control of rain gauge data significantly improves regional sub-daily return level estimates. *Quarterly Journal of the Royal Meteorological Society*, *148*, 1–20. https://doi.org/10.1002/qj.4357

Wallingford HydroSolutions. (2019). The ReFH2 Model. https://refhdocs.hydrosolutions.co.uk/

Wartalska, K., Kaźmierczak, B., Nowakowska, M., & Kotowski, A. (2020). Analysis of hyetographs for drainage system modeling. *Water*, *12*(1), 149. https://doi.org/10.3390/w12010149

Wasko, C., Nathan, R., Stein, L., & O'Shea, D. (2021). Evidence of shorter more extreme rainfalls and increased flood variability under climate change. *Journal of Hydrology*, *603*(PB), 126994. https://doi.org/10.1016/j.jhydrol.2021.126994

Wasko, C., & Sharma, A. (2015). Steeper temporal distribution of rain intensity at higher temperatures within Australian storms. *Nature Geoscience*, *8*(7), 527–529. https://doi.org/10.1038/ngeo2456

Woods Ballard, B., Wilson, S., Udale-Clarke, H., Illman, S., Scott, T., Ashley, R., & Kellagher, R. (2015). The SUDS manual. CIRIA.

Wu, S. J., Yang, J. C., & Tung, Y. K. (2006). Identification and stochastic generation of representative rainfall temporal patterns in Hong Kong territory. *Stochastic Environmental Research and Risk Assessment*, *20*(3), 171–183. https://doi.org/10.1007/s00477-005-0245-5

Yen, B. C., & Chow, V. T. (1983). Local design storm: Volume 1. Executive summary—FHWA/RD-82/063. U.S. Department of Transportation—Federal Highway Administration: Washington D.C.

Yi Ng, J., Fazlollahi, S., & Galelli, S. (2020). Do design storms yield robust drainage systems? How rainfall duration, intensity, and profile can affect drainage performance. *Journal of Water Resources Planning and Management*, *146*(3), 1–13. https://doi.org/10.1061/(ASCE)WR.1943-5452.0001167

Yin, S., Wang, Y., Xie, Y., & Liu, A. (2014). Characteristics of intra-storm temporal pattern over China. *Shuikexue Jinzhan/Advances in Water Science*, *25*(5), 617–624.

Zhu, Z., Wright, D. B., & Yu, G. (2018). The impact of rainfall space-time structure in flood frequency analysis. *Water Resources Research*, *54*(11), 8983–8998. https://doi.org/10.1029/2018WR023550

SUPPORTING INFORMATION

Additional supporting information can be found online in the Supporting Information section at the end of this article.

How to cite this article: Villalobos Herrera, R., Blenkinsop, S., Guerreiro, S. B., Dale, M., Faulkner, D., & Fowler, H. J. (2023). Towards new design rainfall profiles for the United Kingdom. *Journal of Flood Risk Management*, e12958. https://doi.org/10.1111/jfr3.12958

17533318x, 0, Downloaded from https://onlinelibrary.wiley.com/doi/10.1111/jfr3.12958 by Newcastle University, Wiley Online Library on [08/11/2023]. See the Terms and Conditions (https://onlinelibrary.wiley.com/terms-and-conditions) on Wiley Online Library for rules of use; OA articles are governed by the applicable Creative Commons License